Optical properties of epitaxially grown submonolayer CdSe/ZnSe nanostructures

A. M. Kapitonov[1,2] and T. Itoh[1]
[1]*Graduate School of Engineering Science, Osaka University, Toyonaka 560-8531, Japan*
[2]*Institute of Molecular and Atomic Physics, NASB, Minsk 220072, Belarus*

U. Woggon*
Experimentelle Physik IIb, Universität Dortmund, Otto-Hahn-Str. 4, 44221 Dortmund, Germany

D. Kayser and D. Hommel
Institut für Festkörperphysik, Universität Bremen, D-28359 Bremen, Germany
(Received 26 May 2004; published 3 November 2004)

The optical properties of epitaxially grown CdSe/ZnSe nanostructures with nominal CdSe coverage between 0.15 monolayer (ML) and 0.58 ML are investigated by photoluminescence (PL) and PL excitation spectroscopy at low and high excitation density, time-resolved PL, temperature dependent linewidth analysis, and two-photon excitation spectroscopy. We discuss exciton-phonon complexes in a potential and analyze their dominant dimensionality. The exciton-polaron picture, which is mostly applied to the extreme case of very strong exciton-phonon coupling, is introduced here as a well-suited description of the optical properties of ultra-small semiconductor nanostructures with relaxed quantum confinement.

DOI: 10.1103/PhysRevB.70.195304 PACS number(s): 73.22.−f, 78.55.−m, 78.67.−n

I. INTRODUCTION

The interest in artificial semiconductor nanostructures was originally motivated by the fascinating possibility of engineering band structures and hence tuning optical transition energies. These days, the aspect of engineering homogeneous linewidths, *g* factors, fine structure splittings, or optical transition dipole moments gains more and more attention. Optimized nanostructures are being developed that are functional for a specific application or an examination of a particular fundamental problem. One goal, for example, is the creation of quantum structures which have the optimum ratio between long coherence time (low dephasing rates) and large optical transition dipole moment (large extension of the excitonic wave function). Here we present a study of nanometer-sized CdSe inclusions in ZnSe layers which are so-called submonolayer (sub-ML) structures. For these structures the amount of deposited CdSe during epitaxial growth is so low that an uniform quantum well cannot be formed.[1,2] Also the usual quantum dot concepts of three dimensionally, tightly confined electron-hole pairs inside a nanocrystal, or an epitaxially grown island[3] are not applicable. For sub-ML structures made from a strongly polar II-VI compound semiconductor system, the formation of a bound exciton-LO phonon complex (polaron in a potential) is discussed[4] resulting in a strongly modified exciton-phonon interaction, for example, a decoupling of the formed exciton-LO phonon complex from the remaining bath of acoustic phonons. Sub-ML CdSe/ZnSe structures are also interesting materials from the perspective of applications. They emit in the blue-violet spectral range and have been successfully used as an active medium in laser structures.[5,6] A successive energy shift from 2.79 to 2.71 eV and a change in linewidth has been reported when growing ML CdSe/ZnSe nanostructures with nominal layer thicknesses between 0.15 and 1 ML.[7,8] But no systematic study is performed on the photoluminescence excitation spectra, exciton-LO-phonon interaction, high-excitation effects, and influence of continuum states in these systems in relation with the bound exciton-LO phonon complex, hereafter we use the notation CdSe-bound exciton (polaron) to call these states.

In this paper we present a set of experimental data comprising photoluminescence (PL) and PL excitation spectroscopy at low and high excitation density, time-resolved PL, temperature dependent linewidth analysis, and two-photon excitation spectroscopy. We compare two characteristic sub-ML structures with exciton binding energies E_b larger ($E_b > E_{\mathrm{LO}}$) and smaller ($E_b < E_{\mathrm{LO}}$) than the LO-phonon energy E_{LO} of the ZnSe host ($E_{\mathrm{LO}}=31.8$ meV). To explain the peculiar optical properties of sub-ML nanoinclusions, we discuss exciton-phonon complexes in a potential, analyze experimentally the relation with background continuum states, and discuss their dominant dimensionality.

II. SAMPLES

The samples used are CdSe/ZnSe structures with nominal 0.58 and 0.15 ML CdSe coverage. The sample structure is sketched in the inset of Fig. 1. The ZnSe host film is the product of conventional molecular beam epitaxy while migration enhanced epitaxy (MEE) was used to deposit CdSe. A single circle of MEE results in a CdSe layer with a nominal thickness of 0.15 ML. Triple repeating of the MEE process results in the formation of nominally 0.58 ML thick CdSe inclusions. Each sample contains three submonolayers of CdSe which are separated by 18 nm (0.15 ML) or 21 nm of ZnSe spacer layers. Three different sets of GaAs substrates with different crystallographic orientation are examined to grow sub-ML CdSe/ZnSe structures: (001) exactly, 4°, and 10° misoriented with tilt directions towards $\langle 0\bar{1}1\rangle$ (4°) and $\langle 111\rangle$ (10°). A detailed description of the sample

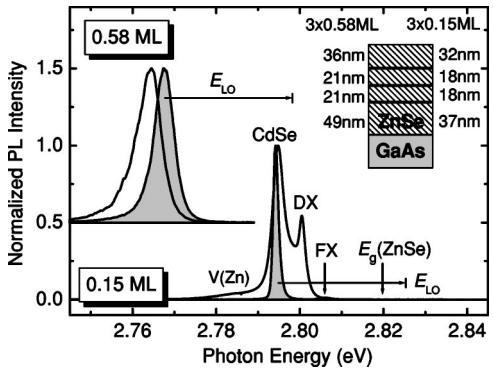

FIG. 1. Normalized PL (photoluminescence) spectra of sub-ML CdSe/ZnSe nanostructures at 4 K. Shadowed curves relate to the samples grown on (001)-oriented GaAs. The spectra of 4° and 10° misorientation of the substrate are shown for 0.58 and 0.15 ML CdSe coverages, respectively. Vertical arrows denote the spectral positions of the ZnSe bandgap (E_g) and the ZnSe free exciton (FX). The length of the horizontal arrows corresponds to the energy (E_{LO}) of the ZnSe LO-phonon. The inset shows the structure of the samples.

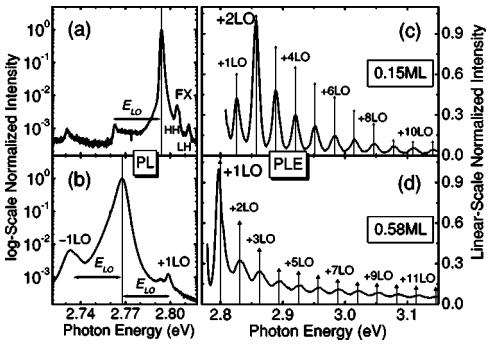

FIG. 2. Normalized photoluminescence (a) and (b) and PL excitation (c) and (d) spectra of 0.15 ML (a) and (c) and 0.58 ML [lower parts (b) and (d)] CdSe/ZnSe nanostructures grown on (001)-oriented GaAs substrates. The length of horizontal arrows (on the left) shows the energy of ZnSe LO-phonon E_{LO}. HH and LH mark the heavy- and the light-hole components of the free ZnSe exciton FX. Vertical arrows (on the right) are set at photon energies which exceed the emission peak energy by an integer multiple of E_{LO}.

growth technique can be found in Refs. 2, 9, and 10. The thicknesses of the ZnSe buffer, spacer, and capping layers provide efficient vertical isolation of the CdSe insertions. The total thickness of the CdSe/ZnSe heterostructure is well below 150 nm, the critical value for the formation of misfit dislocations in thin ZnSe films grown on GaAs.[11] The minimum thickness necessary for the self-aggregation of CdSe into quantum dots is given as 0.5 ML.[12] Due to their diffusive boundaries these dots are more likely to be a local fluctuations of the Cd content in a thin ZnCdSe quantum well.[13] Hence, no growth of structural islands is expected in nanostructures with nominally 0.15 ML deposited CdSe. The deficit of cadmium prevents the formation of a homogeneous layer or island with sharp interfaces which would fit the definition of a quantum well or dot.

As can be seen in Fig. 1, an efficient photoluminescence due to recombination of excitons localized at sub-ML CdSe insertions can be observed which is concentrated in the spectral ranges around 2.76–2.77 eV (0.58 ML) and 2.79–2.8 eV (0.15 ML). The relative shifts of the PL peaks with respect to the characteristic energies of the ZnSe matrix are summarized in Table I along with data from a 2 ML CdSe/ZnSe sample taken from Ref. 13 for comparison. The

TABLE I. Peak energies E, PL-bandwidth at full width at half maximum (FWHM), and energy differences with respect to the ZnSe free exciton energy ΔE(FX) and the ZnSe band gap energy $\Delta E(E_g)$ for samples with different nominal ML thickness of deposited CdSe on ZnSe substrate grown on (001)-oriented GaAs substrates (no misorientation).

Sample (ML)	E (eV)	FWHM (meV)	ΔE(FX) (meV)	$\Delta E(E_g)$ (meV)
0.15	2.794	1.4	12	26
0.58	2.768	5.5	~41	56
2.0	2.58	75	~226	240

PL maximum of the 0.15 ML nanostructure is shifted relatively to the ZnSe free exciton by ~12 meV. This value exceeds the binding energies of excitons bound to Li or Na acceptors in ZnSe and is roughly twice as high as the binding energy of excitons bound to donor impurities such as Al, Ga, etc.,[14] whose chemical nature is more similar to cadmium. Clustering and mutual interaction of Cd atoms deposited as CdSe on ZnSe is very likely, even at extremely low content, close to only 0.1 ML.[15] The size of the ZnSe exciton (Bohr radius a_B=4.4 nm), however, is much larger than the extension of the Cd-rich regions. These facts imply that the excitons in sub-ML CdSe/ZnSe systems can be bound to CdSe inclusions rather than become confined inside them.

In Fig. 1, results for growth on misoriented substrates can also be seen. Growth on such substrates may result in various localized states at stacking faults and in anisotropies in the confining potentials. In our case, the use of a misoriented GaAs substrates leads to a general loss in quantum efficiency and a variation of the peak energy within a more inhomogeneously broadened PL band in the 0.58 ML samples (see Fig. 1). In the spectra of the 0.15 ML nanostructures additional misorientation-induced lines appear with spectral positions similar to that of neutral donor-bound excitons and zinc vacancies in zinc selenide.[11,14]

In the 0.15 ML sample the emission from free excitons FX of the ZnSe host material can be observed [see the PL-spectrum in logarithmic scale in Fig. 2(a)]. Its energy position is influenced by biaxial compressive strain which is unavoidable in high-quality crystalline ZnSe films coherently grown on GaAs substrates.[11] This strain separates and shifts the heavy- (HH) and the light-hole (LH) branches of the upper valence band level of cubic ZnSe toward higher energies. Such a splitting and shift from the bulk ZnSe free exciton (FX) position at 2.802 eV is found for the 0.15 ML samples resulting in additional lines due to both (HH) and (LH) states of the ZnSe host grown on (001)-GaAs at 2.806 and 2.813 eV with a spectral shape strongly distorted by reabsorption and other factors[16] [Fig. 2(a)].

III. RESULTS AND DISCUSSION

A. Optical transitions in emission and excitation spectra of sub-ML CdSe/ZnSe structures

To explore the internal energy level structure, a common method is the measurement of the photoluminescence excitation (PLE) spectrum. Figure 2 shows the PLE spectra of the 0.15 and 0.58 ML sample together with the photoluminescence spectra (in logarithmic scale). The PLE spectra are recorded with a detection energy resonant to the main emission peaks at 2.794 eV for the 0.15 ML sample and 2.768 eV for the 0.58 ML sample by using a Jasco FP-750 spectrofluorometer with a spectral resolution of 1 nm. The PL has been excited by the 325 nm line of a He—Cd laser and detected by a Jobin-Yvon T 64000 triple monochromator equipped with a liquid nitrogen cooled charge-coupled device camera. A gas flow helium cryostat was used to keep the temperature at 3.8 K. The main intriguing features in the optical spectra of the studied sub-ML structures are the following: (i) PLE spectra which have been recorded in resonance to the CdSe-inclusions are composed of equidistant peaks separated by the LO-phonon energy of the ZnSe host material; (ii) no peaks in PLE are found which can directly be attributed to excited electronic states of the confined electron-hole pairs; (iii) the series of LO-phonon-related peaks is more pronounced for the smaller sub-ML structure (up to 15 LO features are resolvable for 0.15 ML CdSe coverage) and extends up to energies high in the continuum above the ZnSe band edge; and (iv) the emission spectrum also shows LO-phonon satellites, however, of much smaller intensity (note the logarithmic scale of PL spectra and linear one of PLE). The strong disparity between the peak intensities in PLE and PL is in clear contradiction to the standard Huang-Rhys model predicting a mirrorlike relation between LO-phonon assisted absorption and emission spectra.

In the PLE spectrum of the 0.58 ML sample, the first peak separated by E_{LO} from the luminescence peak is located at 2.797 eV which is still below the ZnSe band edge ($E_g = 2.82$ eV) and has the ZnSe free exciton FX as a shoulder at 2.805 eV, while for the 0.15 ML sample all peaks in PLE are found above the ZnSe band edge. The logarithmic plot of the PL spectra reveals weak emission lines located at the higher energy side of the main peak. They arise from the free exciton of the thin ZnSe host layer which is split into heavy (HH) and light (LH) hole exciton due to the strain [Fig. 2(a)]. Figure 2(b) shows the emergence of both +1 LO and −1 LO-shifted peaks in the emission spectrum of the 0.58 ML sample. Superimposed on the high-energy (+1 LO) satellite is a small peak at the same energy as that of the 0.15 ML CdSe insertions. Thus, traces of individual MEE cycles occur in sub-ML nanostructures due to incomplete aggregation of deposited cadmium. The PL and PLE spectra plotted in Fig. 2 are completely different from the PL and PLE spectra obtained for a CdSe island embedded in a ZnCdSe quantum well.[13] Comparing the CdSe quantum dots sample with the sub-ML samples, the following trends can be established: (i) The smaller the CdSe submonolayers become, the more the PLE spectra are dominated by the LO-phonon progressions instead of confined exciton excited states and (ii) with decreasing the nominal thickness of CdSe, the LO-phonon progression in emission spectra is dominated by the ZnSe LO phonons and its intensity decreases. For the intensity ratio between principal (or zero-phonon) line (ZPL) and first LO-phonon (1LO) replica, $I_{\mathrm{ZPL}}/I_{\mathrm{1LO}}$, we found 0.035 for the CdSe island, 0.006 for the 0.58 ML sample, and 0.001 for the 0.15 ML sample. The fact that the ZnSe LO phonon is the dominating partner to which the exciton couples in the sub-ML structures is an important hint for the discussion of the problem of dimensionality: The deposited CdSe material is not gathered together to form a nanostructure which is a large assembly such as an island. The grown CdSe nanostructure cannot confine the exciton wave function completely.

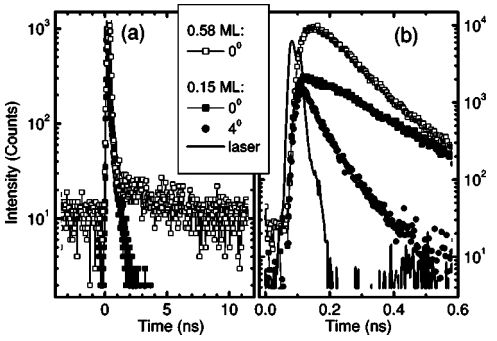

FIG. 3. Luminescence decay kinetics of sub-ML CdSe/ZnSe nanostructures. (a) Time scale covers a 10 ns time range. (b) Time scale for the first 500 ps. Closed symbols: 0.15 ML; open symbols: 0.58 ML. The solid line in (b) shows the response function of the detection system with respect to the laser pulse. The data were obtained after excitation with 10 ps-laser pulses of an attenuated second harmonic from a Ti:sapphire laser and with the detection by a Hamamatsu streak-camera (time resolution of ~30 ps). Taking into account the 80 MHz repetition rate of the excitation pulses, the accumulation effect due to longer life time components is obvious for the 0.58 ML samples, while the luminescence of the 0.15 ML structures is completely decayed before arrival of the next laser pulse.

The gradual transition from a quantum-dot-type structure toward another, but not yet classified, type of confinement is also evidenced by the PL dynamics shown in Fig. 3. The luminescence decay in sub-ML CdSe/ZnSe nanostructures is very sensitive to the CdSe coverage. In Fig. 3(a) we compare the overall dynamics in a 10 ns range for the samples grown on substrates without misorientation. Both of the decay curves start with a similar short-time picosecond decay component (70 to 150 ps) but have different long-time decay components of about 500 ps (0.15 ML) and in the nanosecond range (0.58 ML). The longer nanosecond time constant in the 0.58 ML sample is consistent with the exciton decay time in II-VI quantum dots[17,18] and the dark state lifetime in self-organized CdSe/ZnSe islands.[19] However, such a long component is not observed for the 0.15 ML sample. The clear missing of the long decay component in the 0.15 ML nanostructure indicates the absence of a dark state as usually observed in strongly confined quantum dots as a result of increased exchange interaction. Thus, the exciton in a sub-ML sample does not experience such a strong confine-

ment that the exchange interaction becomes important.

Figure 3(b) shows the initial dynamics within the first 500 ps, in which the data obtained for the samples grown on a misoriented substrate are also included. Lattice imperfections lead to significant luminescence quenching, in particular for the 0.15 ML sample grown on misoriented GaAs wafer. This fact also suggests that the excitons at ultrasmall CdSe inclusions are only weakly localized, in contrast to the strong confinement of excitons in ordinary quantum dots. Weaker localization of the exciton allows faster deactivation via defects whose concentration is increased in samples with misoriented GaAs substrates (see for comparison the PL spectra in Fig. 1).

B. Exciton-Phonon Interaction

Although many reports exist about the luminescence excitation spectroscopy and the exciton-phonon interaction of shallow impurity states in II-VI semiconductors,[11,14,20] neither a systematic state engineering was possible until now, nor have variations in ground-state energies or energy differences between ground, excited, and matrix/host states been explored. A large variety of theoretical descriptions can be found as well[21–24] performed in different levels of approximation. However, how to model theoretically exciton-LO phonon interaction in quantum structures and its dynamics correctly is presently a highly debated problem,[4,25–30] in particular for the range of Fröhlich coupling constants α_C (which gives the relative strength of the electron-LO interaction, see, e.g., Ref. 31) between 0.1 and 1, i.e., in the intermediate coupling regime.

Although the observation of LO-phonon related peaks in PLE is not rare, the number of phonons here is exceptional high. In the past, there have been many attempts to explain such observations. The experimentalists working on quantum dots borrowed such illustrative pictures like the famous Huang-Rhys model for strong electron-phonon interaction. The standard Huang-Rhys approximation describes the interaction of excitons with LO phonons by means of the Huang-Rhys parameter S. This approximation predicts that LO-phonon sidebands have similar Poisson-distributed intensity envelopes both in emission and absorption spectra. Such features were partly found for semiconductor impurities and nanostructures.[31,32] A more detailed theory is developed for various kinds of quantum dots, in which the change in the wave function and coupling strength with confinement and the consequences for the exciton-phonon interaction have been discussed.[25–27,33–35] In polar semiconductors, the effect of optical phonons on excitons can be of particular importance even in the cases of weak coupling strength[21] or shallow potentials.[24]

In bulk materials or quantum wells the phonon-assisted relaxation picture has been established and often used to explain LO-phonon related peaks appearing in PLE. In the old days, the phenomenon was called "hot luminescence"[36] and reported, e.g., for bound and free excitons in II-VI materials. Recently, very similar observations with respect to the effect of LO phonons have been also reported for luminescence of epitaxial nanostructures with CdTe quantum islands.[37] The femtosecond and picosecond dynamics have been described by exciton-phonon scattering. On the other hand, for materials with strong exciton-phonon interaction, the polaron model was established,[22] with good estimates for the extreme case of the coupling strength exceeding considerably $S=1$.

The illustrative model of the exciton polaron, used here, allows a good description of the interaction of photo-induced carriers with phonons in zero-dimensional polar semiconductors. Polaron effects have been observed in CuCl (Ref. 38) and CdSe (Ref. 39) nanocrystals and in InAs/GaAs islands.[27] Excitons in isolated quantum dots are coupled nonadiabatically to phonons.[25] In the bound exciton-polaron model[4] the high-energy sidebands are introduced as the eigenstates of the system.[23] The assumption of a exciton-polaron picture makes recent experiments more plausible and explains the occurence of coherent processes in the ground states while pumping the system at energies nE_{LO} ($n=1,2,\ldots,$) above the exciton resonance.[40] On the other hand, the optical transition probabilities between bound polaron states are expected to become small, in particular, for higher n-LO phonon processes, and cannot explain our present results of strong peak intensities of such higher members which overlap with the ZnSe continuum states. The phonon-assisted relaxation picture would be able to explain that result even if the continuum states are involved, but it would result in a complete decoherence during the multiple scattering events. Additionally, it would require the formation of excitons at a very early stage of time just at the pump energy. This fact, however, is questionable and still subject of intensive discussions. It is not clear, presently, if the number of observed LO-phonon related peaks depends on the experimental condition, such as the relation between pulse width and scattering time. Experiments using cw and pulsed ultra-fast lasers might result in different relative weights of LO-phonon replicae for similar coupling strengths. Furthermore, weak excitation densities might be essential for the observation of these resonances since, their resonance with the ZnSe continuum states implies a possible damping for high carrier densities. So the theory is far from the understanding of the observation of a huge number of LO-phonon replicae in PLE and its dynamics.

In this section we will show further experimental results and discuss our results on the basis of a polaron picture which introduces bound exciton-phonon complexes as the eigenstates of the system. Associated side bands are considered as the excited states of a polaron in a potential.[4,23,28] In the following we will start with the standard procedure to describe exciton-phonon interaction in cw experiments: The analysis of the temperature-dependent linewidth followed by a temperature-dependent analysis of the PLE spectra and a comparison of LO-phonon related peak intensities in one-photon PLE with those in two-photon PLE. We will discuss these data in the context of a bound exciton-polaron concept.

1. Temperature-dependence of the PL-line widths

Figure 4 shows the temperature-dependent linewidths and peak shifts, while the low-temperature line shape was already shown in Fig. 1 (linear scale) and Figs. 2(a) and 2(b) (log scale). The 0.58 ML samples with larger CdSe coverage

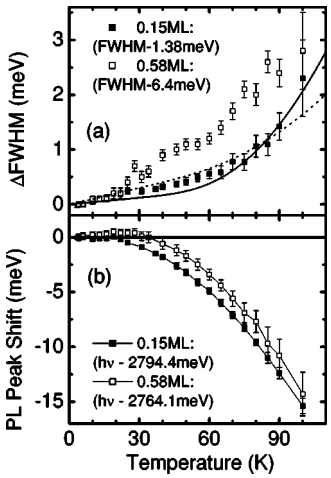

FIG. 4. Spectral broadening (a) and shift (b) of the photoluminescence line of the 0.15 ML CdSe/ZnSe nanostructure grown on (001)-oriented GaAs substrate (solid squares) and of the 0.58 ML CdSe/ZnSe sample with 4° misoriented substrate (open squares). Low-temperature offsets in (a) are FWHM=1.38 meV for 0.15 ML and 6.4 meV for 0.58 ML, with peak maxima at 2.7944 eV for 0.15 ML and at 2.7641 eV for 0.58 ML. The solid line in (a) shows the fit of the FWHM with Eq. (1) using the acoustic (a) and optical (b) phonon coupling coefficients known from bulk ZnSe: $a=4$ μeV/K, $b=65$ meV. The dotted line has been added as an example for a fit with a completely different set of fit parameters: $a=10$ μeV/K, $b=25$ meV (for discussion see text).

exhibit a significant inhomogeneous broadening of the luminescence lines caused by a variation of morphology and, possibly, stoichiometry of CdSe inclusions until quantum dot formation starts. The observed low-temperature line broadening [full width at half maximum (FWHM)] is 5.4 meV for 0.58 ML nanostructures grown on (001) GaAs and 6.4 meV for 4° misoriented substrate. As a result of such inhomogeneous broadening, the temperature dependence of luminescence is shaped by the effect of thermal redistribution of excitons in a potential landscape of varying localization potentials when increasing with temperature the thermal activation energy. Thermal populating of smaller quantum dots is responsible for the high energy shift of the PL peak in the temperature range below 30 K [open squares in Fig. 4(b)]. The inherent effect of thermal redistribution leads to a nearly linear dependence of the observed line width on temperature. The smallest line broadening is found for CdSe inclusions grown on (001)-oriented GaAs substrates. In the case of 0.15 ML CdSe coverage, the PL peak is located at 2.794 eV in the low-temperature limit and its FWHM is less than 1.4 meV. With increasing temperature, the PL peak position follows the shrinking of the band gap of ZnSe matrix [Fig. 4(b), solid symbols]. No obvious spectral redistribution has been observed in case of the 0.15 ML sample. The linewidth of the PL peak remains rather stable in spite of temperature increase until the detrapping of excitons from 0.15 ML CdSe inclusions, as shown in Fig. 4(a).

As can be seen from Fig. 4, the measured temperature-dependent change in the line broadening of the sub-ML samples can hardly be fit by equation

$$\mathrm{FWHM}(T) = \Gamma_0 + aT + \frac{b}{\exp\left(\frac{E_{\mathrm{LO}}}{k_{\mathrm{B}}T}\right) - 1}, \qquad (1)$$

which is a widely used and well-known model for bulk crystals or well-defined quantum wells.[41] We explain the discrepancy by the following reasons: (i) The presence of an inhomogeneous contribution to the total line shape. The low-temperature part of FWHM (T) is clearly influenced by the population statistics and the energy distribution of localized states. This results in an overestimate of the acoustic phonon contribution represented by the coefficient a; (ii) The close band edge allows the population of barrier states and an increase of dephasing from exciton-exciton scattering with increasing temperature may be expected which results in an overestimate of the contribution from optical phonons represented by the coefficient b; and (iii) The fitting procedure does not result in an unambiguous result. As seen in Fig. 4(a), the data for the 0.15 ML sample with only small inhomogeneous broadening can both be fitted to Eq. (1) either by making use of the published parameter $a=4$ μeV/K, $b=65$ meV, and $E_{\mathrm{LO}}=31.8$ meV derived for bulk ZnSe or by a completely different set of parameter ($a=10$ μeV/K, $b=25$ meV). Thus we conclude that such a fit function is not sufficient to analyze the experimental data and a more detailed microscopic model has to be provided.

A more intuitive way to characterize acoustic and optical phonon contributions is obtained by a closer look at the low-temperature line shape with less pronounced inhomogeneous broadening. Figure 2(a) shows the PL line shape of the less inhomogeneously broadened 0.15 ML sample on a logarithmic scale. Comparing with the non-Lorentzian line shape typical for quantum dots[30,42,43] and composed of a sharp Lorentzian line and a broad background associated with acoustic phonons, such a background is present neither at 4 K nor emerges at elevated temperatures (or at least suppressed by two orders of magnitude compared with the case of CdTe islands[44]). From the observed line shape we conclude the suppression of acoustic phonon interaction and the more pronounced coupling to LO phonons in ultrathin sub-ML nanostructures which strongly supports our exciton-LO phonon polaron approach and the assumption of a decoupling of the formed exciton-LO phonon complex from the remaining bath of acoustic phonons.

2. Temperature-dependence of the PLE spectrum

Figure 5 shows the temperature-dependent PLE spectra of the 0.15 ML nanostructure grown on (001)-oriented GaAs wafer with no misorientation. The spectrum maintains its shape with increasing temperature and is essentially the same even if the temperature was varied from 3.5 up to 70 K. Above 60 K a significant (two orders of magnitude) decrease of the luminescence intensity occurs as a result of thermal ionization. The LO-phonon peaks follow the temperature-dependent shift of the emission line and do not get broader. Thus, the behavior of LO-phonon replicae in PLE corresponds well to the principal line observed in PL [Fig. 4(a), solid squares]. No effect of rapidly growing population of acoustical phonons has been observed, while the kinetic ap-

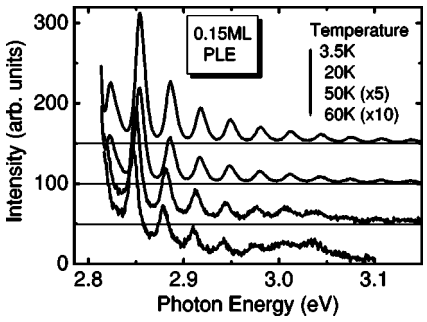

FIG. 5. PLE spectra measured at temperatures of 3.5, 20, 50, and 60 K. The sample grown on (001)-oriented GaAs substrate contains CdSe inclusions of nominal thickness of 0.15 ML. The detection energy is adjusted to follow the temperature-dependent shift of the maximum of the luminescence peak. The spectra are shifted vertically for clarity and the corresponding zeroth levels are visualized with horizontal lines. The numbers in parentheses show the factors of magnification.

proach predicts faster thermalization of "hot" excitons at elevated temperatures.

3. Two-photon excitation spectrum

A drastic modification of the PLE spectra was observed when using two-photon excitation (TP-PLE), as illustrated by Fig. 6. First, no emission enhancement was observed when the two-photon excitation energy is tuned in resonance with the luminescence peak. On the contrary, such a resonant increase of the emission intensity was clearly observed in the case of one-photon excitation. This behavior can be interpreted in favor of *s*-type symmetry of the envelope part of the wave function describing the ground state of the bound polaron. Second, the modulation of the PLE signal with the LO-phonon sequence is eliminated in the TP-PLE spectrum

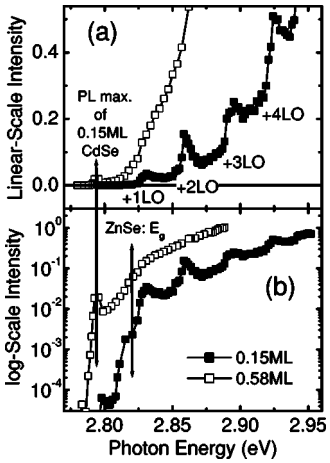

FIG. 6. Two-photon PLE spectra of CdSe/ZnSe nanostructures grown on (001)-GaAs. Nominal CdSe coverage is 0.15 ML (solid squares) and 0.58 ML (open squares). The vertical scale is linear in (a) and logarithmic in (b). The position of the ZnSe band gap and the PL peak of the 0.15 ML sample are marked by arrows. The excitation source is a mode-locked Ti:sapphire laser with 3 ps pulse width, 80 MHz repetition rate, and 60 mJ/s average power.

of the 0.58 ML sample (open symbols). Two minor features which do exist must be associated with the band gap of ZnSe host and with residual ultra-small CdSe inclusions. In the case of 0.15 ML coverage the series of LO satellites is somewhat suppressed but still existing. One must consider the effects of various lattice modes, direct relaxation into the exciton ground state, etc., in order to explain the much closer similarity between two-photon PLE spectra and that of two-photon absorption by the ZnSe host [the latter contribution is proportional to $(2\hbar\omega - E_g)^{3/2}$ (Ref. 45) instead of $(\hbar\omega - E_g)^{1/2}$ in the one-photon case]. From the data of Fig. 6 we see how sensitive the contribution of LO phonons in the process of energy relaxation depends on the symmetry of the elementary photoinduced excitations. Within the bound exciton-polaron model, this fact is an evidence of the existence of selection rules for transitions involving polaronic eigenstates. On the contrary, the use of the so-called kinetic energy relaxation picture will demand an essentially more complicated microscopic picture rather than the simple approach of the Markovian "hot" exciton relaxation[46] due to the random LO-phonon scattering, and is not appropriate in our case.

C. High-excitation effects and the influence of continuum states

The observation of up to 15 equidistant PLE-peaks at energies highly above the ZnSe-band edge $E_g = 2.82$ eV, i.e., resonant to the continuum states of ZnSe with peak heights and line shapes extremely sensitive to the sub-ML coverage calls for a more detailed study of the continuum contribution to the PLE-signals, i.e., the study of PLE under high excitation.

To examine the optical properties of sub-ML CdSe/ZnSe nanostructures under high excitation conditions, pulsed tunable lasers are used as optical pump sources. The PLE spectrum for the 0.15 ML sample under pulsed excitation of high carrier densities with a spectrally tunable Coumarin 440 dye laser (10 ns pulse width, 3 μJ pulse energy, 10 Hz repetition rate) is shown in the upper part of Fig. 7. The ordinate of each data point is proportional to the spectrally integrated luminescence intensity normalized by the power of the laser at the given wavelength. The lower part of Fig. 7 shows the emission spectra at different pump intensities excited by the second harmonic of a Ti:sapphire laser (3 ps pulse width, 80 MHz repetition rate, maximum 360 pJ/pulse energy).

Both PL and PLE spectra undergo dramatic changes under high pump power (compare with Fig. 2). In the PLE spectrum, the LO-phonon maxima completely disappear. The single sharp feature, which totally dominates the high-excitation PLE spectrum, arises from heavy-hole free excitons excited in the ZnSe barrier. At higher excitation energies, the spectrum becomes flat and structureless. Simultaneously to the pump-induced disappearance of the LO-phonon related features in the PLE spectrum, the apparent elimination of Raman signals in the emission spectrum is observed. The changes in the emission spectrum with increasing pump intensity have been measured by use of a picosecond laser as shown in Fig. 7 (the topmost curve is

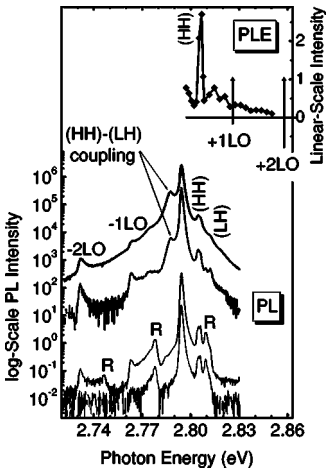

FIG. 7. Upper part: High-excitation PLE spectrum of the 0.15 ML CdSe/ZnSe nanostructure [(001)-GaAs substrate] recorded by using a 10 ns-pulsed Coumarin 440 dye laser with 10 Hz repetition rate and 3 μJ/pulse energy as the excitation source. Vertical arrows mark the energies expected for the first two LO-phonon satellites. Lower part: PL spectra of the same sample for different excitation levels from top to bottom: 30 mW (0.36 nJ/pulse), 3 mW, 30 μW, and 3 μW of the second harmonic of a mode-locked Ti:sapphire laser (constant excitation spot of about 0.1 mm^2). The pump pulse photon energy of 2.8735 eV is close to the energy of the +2.5 LO minimum in the low-intensity PLE spectrum of Fig. 2(c) Raman peaks are denoted with "R."

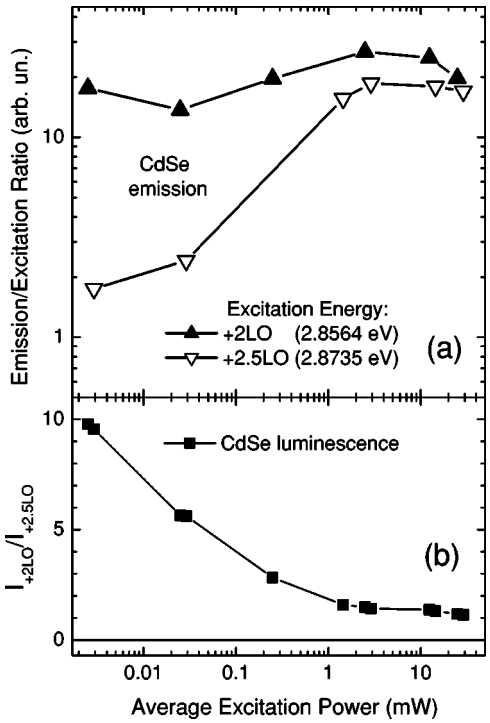

FIG. 8. (a) Emission intensity divided by excitation intensity and plot versus excitation intensity for the luminescence of excitons in a shallow potential of 0.15 ML CdSe inclusions. Solid triangles correspond to the excitation energy 2.8564 eV close to the +2 LO maximum and open triangles to 2.8735 eV in the vicinity of the +2.5 LO minimum (as in Fig. 7) of PLE spectrum shown in Fig. 2(c). (b) Ratio of the PL intensity measured with excitation energies fixed at either +2 LO or +2.5 LO calculated from the data sets shown in (a).

similar to the luminescence observed under nanosecond-dye laser excitation used to obtain the PLE spectrum depicted in the inset). While at low excitation levels the Raman replicae of the laser line are easily to resolve, they are covered by the broadened PL peaks when increasing the excitation intensity. At high pump power, an emission peak appears energetically 6.7 meV below the principal PL line. The energy separation coincides with the value of the (HH)-(LH) splitting in the 0.15 ML CdSe/ZnSe nanostructure grown on (001)-GaAs. This line increases superlinearly with increasing excitation intensity due to inelastic exciton scattering.

To explain the difference between the PLE spectra at high and low pump power, there are two hypothetic possibilities: The reduction of the intensity of the LO-replicae or the filling of the dips between the LO-maxima. In order to trace back the evolution of the PLE spectrum with increasing pump power, two different sets of intensity-dependent emission spectra were measured using two fixed excitation energies: (i) The photon energy is with 2.8564 eV close to the most intense +2 LO maximum in the low-intensity PLE and (ii) the photon energy is 2.8735 eV and corresponds to the nearest +2.5 LO minimum. Both cases are summarized in Fig. 8(a) where the data points present the integral luminescence intensity normalized by the power of laser excitation. In this representation, constant conversion efficiency would result in a horizontal line while negative (positive) slope would correspond to the saturation (superlinear growth) of luminescence with pump power. As can be clearly seen in Fig. 8(a), the PL spectrum is sensitive to the combination of excitation photon energy and pump power. When the laser wavelength is off resonance (i.e., tuned to an energy +2.5 LO above the main PL peak energy) the total luminescence signal is always weaker than for on-resonance pumping at +2 LO. But the difference gets smaller and smaller with increasing excitation intensity. At the highest pump power, the emission signal no more depends on the excitation photon energy and reaches almost equal values both for the pumping with +2 LO and +2.5 LO excess energy. The gradual decrease of the E_{LO}-modulation of the PLE spectrum with increasing pump power is shown directly in Fig. 8(b) which displays the ratio of the PL-peak emission intensities under excitation with +2 LO and +2.5 LO excess in the photon energy. Thus, the filling of the +2.5 LO minimum in the PLE spectrum of the 0.15 ML sample occurs when the average laser power increases up to the order of milliwatt (per 0.1 mm^2). This fact indicates that the increase in free carrier density opens an opportunity to capture nonresonant (electron-hole) pairs from ZnSe continuum states into the sub-ML CdSe inclusions. At several mW average excitation power the resonance enhancement effect arising from the exciton-polaron eigenstates is suppressed and mainly dumped by exciton-exciton scattering. Weak confinement and relatively wide spread of the wave function of the bound exciton polaron hardly preserve them from being coupled with another yet delocalized excitons. The (HH-LH)-labeled peak is simultaneously observed, which is caused by inelastic exciton collisions leading to the up conversion of some

fraction of (HH) states to (LH) ones at the expense of the energy of emitted photons (see Fig. 7). This is a further evidence that even at an average laser power of some hundred of μW the concentration of free (HH)-type excitons in the ZnSe host is significantly large and the exciton-exciton collisions dominate the relaxation dynamics.

D. Dimensionality

In this section we address the question of how the confinement has to be classified if the size of the CdSe inclusions gets smaller and smaller. The dimensionality for a sub-ML nanostructure might be either zero-dimensional (localized excitons in sub-ML CdSe inclusions), two-dimensional (2D) (a quantum well of CdZnSe mixed crystal), or bulklike (a ZnSe crystal formed as the total sum of all layers with Cd-related impurities). Because of our growth conditions, all Cd content is concentrated in a nominal 2D layer which is definitely thinner than the characteristic exciton size and exciton percolation along these layers is favored. Since the confining potential is only weak, the confined states are shallow bound states without a pronounced ladder of excited electronic states. The CdSe-bound excitons interact effectively with the ZnSe matrix.

A widely used compromise to describe dimensionality is a quantum well model with implicitly introduced phenomenological averaging parameters.[1,47] The intrinsic inhomogeneity of the layer is referred to as statistical fluctuations in solid solutions. Bound states similar to localized excitons in quantum wells with pronounced well-width fluctuations[48,49] are expected for sub-ML samples with the difference, however, that the thickness fluctuations are less important than the chemical content fluctuations. The decrease of CdSe coverage facilitates the spread of the relative motion of the CdSe-bound exciton into the ZnSe host where the free exciton size ($2a_B$=8.8 nm) is much larger than the thickness of the Cd-rich layer ($\sim$1 nm). In ultra-small sub-ML nanostructures, the binding potential does not depend on the geometry (thickness) of the layer while the coupling with the substrate is important, and thus a 2D-like quantum well model is no more valid. On the other hand, a consideration of a quantum well with randomly varying parameters,[50] e.g., results in diverging cases of strong and weak 3D confinement, delocalized excitons, and even free-exciton resonances above the mobility edge. Rather promising for the sub-ML heterostructures is the fractional-dimensional model,[51] but up to now it was applied mostly to thicker layers.[52]

Our tools to classify the dimensionality are purely optical: The line shape and intensities of the LO-phonon replicae in emission spectra, the presence or absence of multiexcitonic bound states, and the strength of the exchange interaction.

Arguments against the strongly confined "quantum dot"-model are the absence of a fine structure splitting due to exchange interaction (no dark-state dynamics is observed for the 0.15 ML sample) and small biexciton binding energy which, in case of strong confinement, should rather be enhanced.[3] Within our spectral resolution, no biexciton signatures are observed.

Another measure of the effective dimensionality is the analysis of the intensity and line shape of LO-phonon replicae in emission. In Fig. 9 the first (−1 LO) and the second (−2 LO) LO-phonon satellites compared with the principal (so called zero-phonon) PL line are plotted both for the 0.58 and 0.15 ML CdSe/ZnSe nanostructures grown on (001)-GaAs substrate. The PL is excited by the attenuated 441.6 nm line of a He-Cd laser. This wavelength is nearly in resonance with the free exciton states of the ZnSe matrix. In the figure, the LO satellites are shifted in energy exactly by that energy value which was measured for the spectral interval between the Raman replicae of the laser line. The intensities are magnified for the sake of clarity by the factors as depicted. For bulk semiconductors it is well established[53] that delocalized free excitons, in particular in ZnCdSe solid solutions[54] of high crystal quality, exhibit peculiar intensity distribution and profiles for LO-phonon-assisted PL lines. Namely, the first (−1 LO) satellite corresponds to the Fröhlich-type forbidden process while the second (−2 LO) one is allowed. The finite values of the kinetic energy and of the quasimomentum of excitons cause also some high-energy shift ($\sim$kT, thermal energy) of the peaks of LO satellites in PL spectra. Their line shape is asymmetrical with steeper slope on the lower energy side. All these features do occur to some extent in the case of 0.15 ML nanostructure [see Fig. 9(a)]. The peak ratio $I_{-1\ \mathrm{LO}}/I_{-2\ \mathrm{LO}}$ is less than 2. Such small value denies direct comparison with the Huang-Rhys model which would result in a huge overestimate of LO-phonon

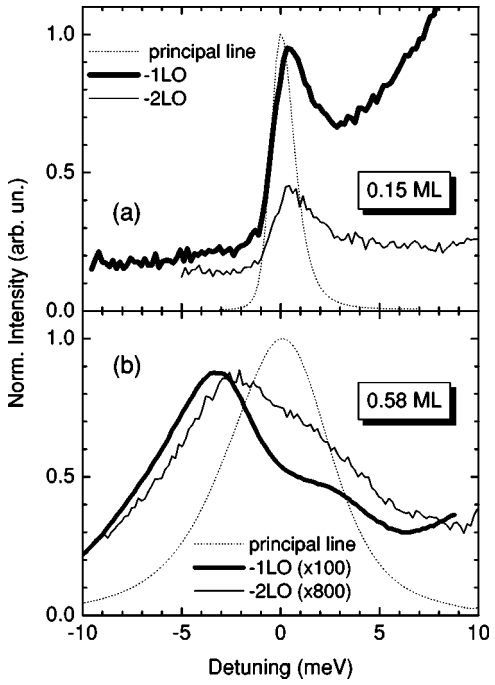

FIG. 9. Spectral profiles of the principal (or zero-phonon line: dotted) and its first (−1 LO: thick line) and second (−2 LO: thin line) LO satellites in the luminescence of 0.15 ML (a) and 0.58 ML (b) CdSe/ZnSe nanostructures grown on (001)-oriented GaAs wafer. The phonon side bands are scaled up by 1000 (a) and by 100 [−1 LO in (b)] and by 800 [−2 LO in (b)] in order to optimize the visibility. The energy "zero" corresponds to the maximum of the main PL line. The satellites are moved toward the "zero" by a corresponding number of E_{LO} derived from Raman replicae of the excitation source, a He-Cd laser operated at 441.6 nm.

coupling. The excitons here are only weakly localized in shallow potentials of the smallest sub-ML epitaxial inclusions.

For the 0.58 ML sample the 3D wave vector selection rules have no effect on the more quantum dotlike states [see Fig. 9(b)] The ratio $I_{-1\ \mathrm{LO}}/I_{-2\ \mathrm{LO}}$ is approximately one order of magnitude higher and depends on the exact energy position within the inhomogeneous spectrum of zero-phonon line (ZPL).[55] The exciton states at the low-energy side of the ZPL are strongly localized and can conform to the model of quasi-0D states. Their LO replicae are relatively strong and go down successively with the number of emitted LO phonons. For the high-energy components of the ZPL the LO satellites are less intense and, moreover, suppressed in the first order (−1 LO) due to the finite velocity of excitons in the weakly localized and extended states. The difference in LO-phonon coupling is responsible for the apparent low-energy shift of the inhomogeneous LO-phonon assisted PL lines of the 0.58 ML sample. Thus, the simultaneous recombination of the very differently confined excitons occurs in the nanostructure with 0.58 ML nominal thickness of CdSe insertions.

IV. SUMMARY

The optical properties of epitaxially grown sub-ML CdSe/ZnSe nanostructures have been examined for varying CdSe ML-coverage. Nanostructures with nominal CdSe coverage of 0.58 ML (and larger) can still be described within the standard model of a strongly, three-dimensionally confined quantum dot. For nanostructures with only 0.15 ML CdSe coverage, the extension of the excitonic wave function into the ZnSe matrix and a reduction of the effect of quantum confinement are reflected in the optical properties. High polarity of both the ZnSe host material and of the CdSe inclusions results in the formation of exciton-phonon complexes, called bound exciton polarons. The PLE spectra consist of a series of intensive LO replicae of the zero-phonon line while LO-phonon related peaks in emission are three to four orders of magnitude weaker. The polaron approach, applied here to ultrasmall inclusions in the host ZnSe crystal, explains the whole spectrum as eigenstates whose energies fit well the experimental data. The static nature of this model does not allow us, however, any prediction on the relaxation dynamics of these quasiparticles. But the observed temperature stability of the PLE spectra, the presence of symmetry-dependent selection rules, etc., can be treated as additional indirect proof of the reality of polaronic eigenstates. The alternative, so-called kinetic picture, takes into account a fast relaxation of excitons as the result of emission of LO phonons. Such a perturbative treatment of the LO-phonon coupling cannot provide any information on the nature of the intermediate states of "hot" excitons. It is based on the assumption of an instantaneous formation of excitons resonant to any pump energy. From our data analysis we conclude that this description is less illustrative compared to the concept of exciton-polaron transitions. Eventually, we hope that the presented data sets help to stimulate more detailed theory work to clarify the nature of exciton-phonon interaction in sub-ML structures. Another topic which needs to be studied in the future is the resonant interaction of discrete polaronic states with a continuum of delocalized states in the semiconductor matrix. In the regime of high excitation, the high carrier density gives rise to multiparticle scattering in sub-ML nanostructures. The interaction with delocalized excitons ranks over phonon effects and such phenomena like the Fano effect, autoionization, etc., must become observable.

ACKNOWLEDGMENTS

This work was supported by the Japan Society for the Promotion of Science (JSPS) and Grant-in-Aid for Scientific Research from Ministry of Education, Culture, Sports, Science and Technology of Japan. The authors are grateful to Professor B. Gerlach (Universität Dortmund), Professor W. Schäfer(†), and Dr. F. Kalina (both Forschungszentrum Jülich) for stimulating discussions.

*Electronic address: ulrike.woggon@uni-dortmund.de

[1] I. L. Krestnikov, N. N. Ledentsov, A. Hoffmann, and D. Bimberg, Phys. Status Solidi A **183**, 207 (2001).

[2] T. Passow, H. Heinke, D. Kayser, K. Leonardi, and D. Hommel, J. Cryst. Growth **214/215**, 606 (2000).

[3] U. Woggon, *Optical Properties of Semiconductor Quantum Dots* (Springer, Berlin, 1997).

[4] U. Woggon, D. Miller, F. Kalina, B. Gerlach, D. Kayser, K. Leonardi, and D. Hommel, Phys. Rev. B **67**, 045204 (2003).

[5] N. N. Ledentsov, I. L. Krestnikov, M. V. Maximov, S. V. Ivanov, S. L. Sorokin, P. S. Kop'ev, Zh. I. Alferov, D. Bimberg, and C. M. Sotomayor-Torres, Appl. Phys. Lett. **69**, 1343 (1996).

[6] I. L. Krestnikov, M. Strassburg, M. Caesar, A. Hoffman, U. W. Pohl, D. Bimberg, N. N. Ledentsov, P. S. Kop'ev, Zh. I. Alferov, D. Litvinov, A. Rosenauer, and D. Gerthen, Phys. Rev. B **60**, 8695 (1999).

[7] S. V. Ivanov, A. A. Toropov, T. V. Shubina, S. V. Sorokin, A. V. Lebedev, I. V. Sedova, P. S. Kop'ev, G. R. Pozina, J. P. Bergman, and B. Monemar, J. Appl. Phys. **83**, 3168 (1998).

[8] S. V. Ivanov, A. A. Toropov, S. V. Sorokin, T. V. Shubina, I. V. Sedova, A. A. Sitnikova, P. S. Kop'ev, Zh. I. Alferov, H.-J. Lugauer, G. Reuscher, M. Keim, F. Fischer, A. Waag, and G. Landwehr, Appl. Phys. Lett. **74**, 498 (1999).

[9] T. Passow, H. Heineke, T. Schmidt, J. Falta, A. Stockmann, H. Selke, P. L. Ryder, K. Leonardi, and D. Hommel, Phys. Rev. B **64**, 193311 (2001).

[10] T. Passow, K. Leonardi, H. Heineke, D. Hommel, D. Litvinov, A. Rosenauer, D. Gerthsen, J. Seufert, G. Bacher, and A. Forchel, J. Appl. Phys. **92**, 6546 (2002).

[11] J. Gutowski, N. Pressler, and G. Kudelek, Phys. Status Solidi A **120**, 11 (1990).

[12] N. Peranio, A. Rosenauer, D. Gerthsen, S. V. Sorokin, I. V. Se-

dova, and S. V. Ivanov, Phys. Rev. B **61**, 16015 (2000).
[13] F. Gindele, U. Woggon, W. Langbein, J. M. Hvam, K. Leonardi, D. Hommel, and H. Selke, Phys. Rev. B **60**, 8773 (1999); F. Gindele, K. Hild, W. Langbein, and U. Woggon, *ibid.* **60**, R2157 (1999).
[14] P. J. Dean, D. C. Herbert, C. J. Werkhoven, B. J. Fitzpatrik, and R. N. Bhargava, Phys. Rev. B **23**, 4888 (1981).
[15] A separate cadmium atom in a bulk ZnSe crystal tends to be an isoelectronic substitution whose potential well is too small to form a localized state (isoelectronic trap). At very low cadmium concentration, the formation of a locally varying $Cd_xZn_{1-x}Se$ alloy is very likely with a modification in x and geometry only. Further increase of Cd content leads to the partial phase separation with the initiation of quantum dot formation. During the epitaxial growth, some Cd atoms might be built-in into any non-equilibrium site making them capable to bind excitons.
[16] A. L. Gurskii, Yu. P. Rakovich, E. V. Lutsenko, A. A. Gladyshchuk, G. P. Yablonskii, H. Hamaden, and M. Heuken, Phys. Rev. B **61**, 10314 (2000).
[17] G. Schlegel, J. Bohnenberger, I. Potapova, and A. Mews, Phys. Rev. Lett. **88**, 137401 (2002).
[18] A. M. Kapitonov, A. P. Stupak, S. V. Gaponenko, E. P. Petrov, A. L. Rogach, and A. Eychmüler, J. Phys. Chem. B **103**, 10109 (1999).
[19] B. Patton, W. Langbein, and U. Woggon, Phys. Rev. B **68**, 125316 (2003).
[20] A. Nakamura and C. Weisbuch, Solid-State Electron. **21**, 1331 (1978).
[21] Y. B. Levinson and E. I. Rashba, Rep. Prog. Phys. **36**, 1499 (1973).
[22] S. Nakajima, Y. Toyozawa, and R. Abe, *The Physics of Elementary Excitations* (Springer-Verlag, Berlin, 1980).
[23] B. Gerlach and F. Kalina, Phys. Rev. B **60**, 10886 (1999).
[24] E. Ya. Sherman, Phys. Rev. B **67**, 014304 (2003).
[25] V. M. Fomin, V. N. Gladilin, J. T. Devreese, E. P. Pokatilov, S. N. Balaban, and S. N. Klimin, Phys. Rev. B **57**, 2415 (1998); E. P. Pokatilov, S. N. Klimin, V. M. Fomin, J. T. Devreese, and F. W. Wise, *ibid.* **65**, 075316 (2002).
[26] D. V. Melnikov and W. B. Fowler, Phys. Rev. B **64**, 195335 (2001); D. V. Melnikov and W. B. Fowler, *ibid.* **64**, 245320 (2001).
[27] S. Sauvage, P. Boucaud, R. P. S. M. Lobo, F. Bras, G. Fishman, R. Prazeres, F. Glotin, J. M. Ortega, and J. M. Gérard, Phys. Rev. Lett. **88**, 177402 (2002); O. Verzelen, R. Ferreira, and G. Bastard, *ibid.* **88**, 146803 (2002).
[28] A. M. Kapitonov, U. Woggon, K. Leonardi, D. Hommel, K. Edamatsu, and T. Itoh, Phys. Status Solidi B **238**, 317 (2003).
[29] F. Rossi and T. Kuhn, Rev. Mod. Phys. **74**, 895 (2002).
[30] B. Krummheuer, V. M. Axt, and T. Kuhn, Phys. Rev. B **65**, 195313 (2002).
[31] K. W. Böer, *Survey of Semiconductor Physics*. 2nd ed. (Wiley, New York, 2002), Vol. 1.
[32] A. D. Yoffe, Adv. Phys. **50**, 1 (2001).
[33] S. Schmitt-Rink, D. A. B. Miller, and D. S. Chemla, Phys. Rev. B **35**, 8113 (1987).
[34] T. Takagahara, J. Lumin. **70**, 129 (1996).
[35] T. Takagahara, Phys. Rev. B **60**, 2638 (1999).
[36] For an early review, see S. Permogorov, Phys. Status Solidi B **68**, 9 (1975).
[37] T. Okuno, M. Nomura, Y. Masumoto, Y. Terai, Sh. Kuroda, and K. Takita, J. Phys. Soc. Jpn. **71**, 3052 (2002).
[38] T. Itoh, M. Nishijima, A. I. Ekimov, C. Gourdon, Al. L. Efros, and M. Rosen, Phys. Rev. Lett. **74**, 1645 (1995).
[39] R. W. Meulenberg and G. F. Strouse, Phys. Rev. B **66**, 035317 (2002).
[40] T. Flissikowski, A. Hundt, M. Lowisch, M. Rabe, and F. Henneberger, Phys. Rev. Lett. **86**, 3172 (2001).
[41] S. Rudin, T. L. Reinecke, and B. Segall, Phys. Rev. B **42**, 11218 (1990); S. Rudin, and T. L. Reinecke, *ibid.* **66**, 085314 (2002); B. Segall, in *Proceedings of the IXth Conference on the Physics of Semiconductors, Moscow, 1968*, edited by S. M. Ryvkin (Nauka, Leningrad, 1968) p. 425.
[42] K. Takemoto, B.-R. Hyun, and Y. Masumoto, Solid State Commun. **114**, 521 (2000).
[43] P. Borri, W. Langbein, S. Schneider, U. Woggon, R. L. Sellin, D. Ouyang, and D. Bimberg, Phys. Rev. Lett. **87**, 157401 (2001).
[44] L. Besombes, K. Kheng, L. Marsal, and H. Mariette, Phys. Rev. B **63**, 155307 (2001).
[45] N. G. Basov, A. Z. Grasyuk, I. G. Zubarev, V. A. Katulin, and O. N. Krokhin, Zh. Eksp. Teor. Fiz. **50**, 551 (1966) [Sov. Phys. JETP **23**, 366 (1966)].
[46] Some deviation from this semiclassical picture was also observed on a femtosecond time scale where the uncertainty relation prohibits consideration of eigenstates with discrete energy spectrum. For reference, see Ref. 29.
[47] A. A. Toropov, S. V. Ivanov, T. V. Shubina, S. V. Sorokin, A. V. Lebedev, A. A. Sitnikova, P. S. Kop'ev, M. Willander, G. Pozina, P. Bergman, and B. Monemar, Jpn. J. Appl. Phys., Part 1 **38**, 566 (1999).
[48] D. Gammon, E. S. Snow, B. V. Shanabrook, D. S. Katzer, and D. Park, Phys. Rev. Lett. **76**, 3005 (1996).
[49] S. Yamaguchi, H. Kurusu, Y. Kawakami, S. Fujita, and S. Fujita, Phys. Rev. B **61**, 10303 (2000).
[50] A. V. Kavokin, Phys. Rev. B **50**, 8000 (1994).
[51] X. F. He, Phys. Rev. B **43**, 2063 (1991).
[52] A. Thilagam, Phys. Rev. B **63**, 045321 (2001).
[53] *Excitons*, Edited by E. I. Rashba and M. D. Sturge (North-Holland, Amsterdam, 1982).
[54] S. A. Permogorov, A. Yu. Naumov, L. N. Tenishev, A. N. Reznitskiĭ, and D. L. Fedorov, Fiz. Tverd. Tela (S.-Peterburg) **37**, 2466 (1995) [Phys. Solid State1 **37**, 1350 (1995)].
[55] The apparent doublet structure of the LO-phonon assisted luminescence satellites of the 0.58 ML sample is due to the occurence of CdSe-type phonons with energy 26.5 meV. Similar splitting into 31.8 and 26.5 meV modes was also observed in the resonant hyper-Raman scattering spectrum of 0D-like states in this sample.